Electronic Supplementary Material (ESI) for Physical Chemistry Chemical Physics.

Bacteriorhodopsin based non-magnetic spin filters for biomolecular spintronics

Vaibhav Varade,[1] Tal Markus,[1] Kiran Vankayala,[1] Noga Friedman,[2] Mordechai Sheves,[2] David H. Waldeck,[3] Ron Naaman[1*]

1. Department of Chemical Physics, Weizmann Institute of Science, Rehovot, Israel

2. Department of Organic Chemistry, Weizmann Institute of Science, Rehovot, Israel

3. Department of Chemistry, University of Pittsburgh, Pittsburgh, Pennsylvania 15260, USA

*Email: ron.naaman@weizmann.ac.il

Supporting Information

Film characterization and device fabrication with OTR-bR

The adsorbed films of OTG-bR were supported on gold and characterized using polarization modulation-infrared reflection absorption spectroscopy (PMIRRAS) and atomic force microscopy (AFM) measurements. Topography images of the bare Au and OTG-bR modified Au substrates were acquired in tapping mode using an AIST-NT smart SPM. Commercial Pt coated Si tips (HQ: DPE XSC11, Mikromasch) were used. Topography scans were performed at a scan rate of 1 Hz over different regions of the sample. As shown in Fig. S1(a) and S1(b), a clear difference in the surface topography between bare and OTG-bR modified Au surface confirms the presence of OTG-bR monolayer. The thickness of OTG-bR films adsorbed on Au was measured using the nanoshaving technique as shown in Fig. S1(c). A designated area was scanned in contact

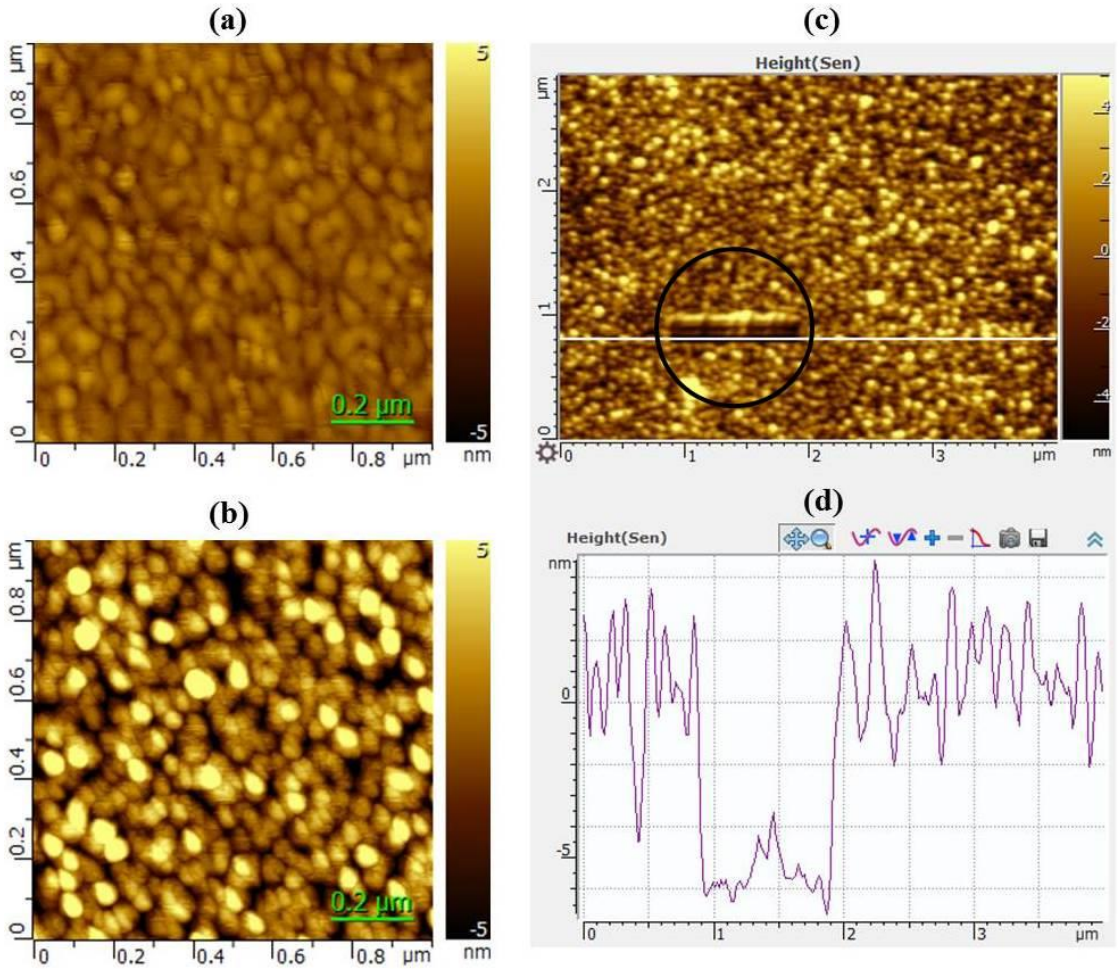

Fig. S1: (a) Topographic scan of clean Au surface on glass substrate; (b) topographic image of OTG-bR SAM on Au surface; (c) topographic image depicting nanoshaving (encircled) technique; and (d) height scan profile for the OTG-bR SAM.

mode at a high tip-loading force in order to remove OTG-bR molecules from the surface. Fig. S1(d) gives the cross-section line profile, along the shaved region, and yields a thickness of ~ 6 nm.

Details of the Au/cysteamine/OTG-bR/MgO/Ni devices

The Au/Cy/OTG-bR/MgO/Ni devices were fabricated with the chiral SAM on a Au electrode as the injector and a ferromagnetic top contact of Ni was evaporated onto the MgO as the polarization analyzer. The devices were created in a cross geometry. Au lines of 1 micron width were patterned using photolithography and deposited via e-beam evaporation (80 nm Au on 8 nm Ti as adhesion layer) onto a glass substrate cleaned with acetone, iso-propyl alcohol, and plasma etching. Au surfaces were cleaned thoroughly using a UV-plasma, followed by washing with warm ethanol. The cleaned Au surfaces were immediately immersed in a 5 mM solution of cysteamine in ethanol for 2 hours. Note that growing a cysteamine SAM on Au requires high precision, in terms of the solution concentration and time of adsorption, to avoid the etching of the gold by the molecules. In the following step, a buffered solution of OTG-bR was dropcast on the cysteamine/Au surfaces. The samples were kept in a closed wet environment to avoid drying for 30 minutes. Thereafter, the substrates were washed very gently and were left in deionized water for 12 hours in order to open the vesicles attached to the bR. The substrates were dried and 2.5 nm of MgO was deposited by e-beam evaporation in a vacuum of about 10^{-6} mbar at the rate of 10 pm/s. In the final step, a 150 nm thick layer of Ni was evaporated on to the Au lines with OTG-bR in a cross geometry structure.

Wild type bR adsorption

Fig. S2 shows the scanning electron microscopy image of drop-casted WT-bR on a clean gold surface. It can be seen that WT-bR forms patches of different sizes, varying from submicron to more than tens of micron. It was quite difficult to get reproducible

magnetoresistance (MR) results from spin valves made from drop-casted WT-bR because of pinholes and the yield from the number of devices was limited to ~5%.

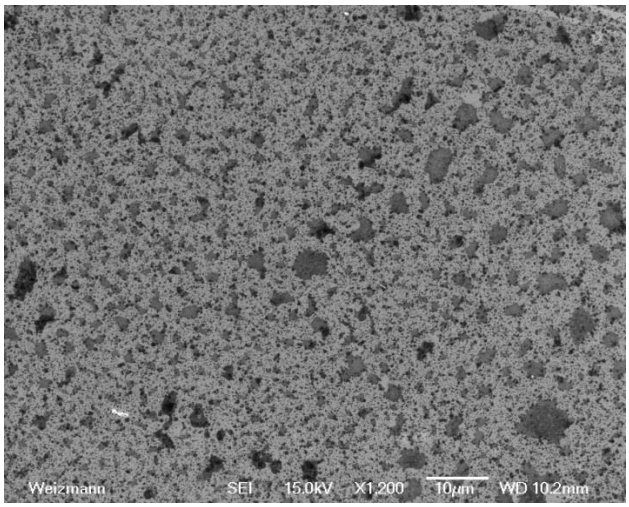

Fig. S2 SEM image of drop casted wild-type bR on gold surface

Fig. S3 shows the MR percentage as a function of applied external magnetic field from -1 T to +1 T at different temperatures varying from 300 K to 120 K. Typical antisymmetric MR curves have been obtained. This is the key feature of CISS based spin valves with one ferromagnetic analyzer. The net change in MR between the low and high resistance states is around ~0.8 %, and this value is basically temperature independent. The shapes of curves vary at low temperature due to possible conformational changes of the WT-bR at low temperature. In this case 2 nm of alumina was deposited on to the WT-bR layer by an atomic layer deposition (ALD) process at 100 ^{o}C. This could also be a reason for the low yield of device because it is known that alumina is mostly amorphous when deposited at low temperatures i.e. < 200 ^{o}C. The best alumina layer is usually formed at 250 ^{o}C, however at this temperature the bio-system is damaged severely.

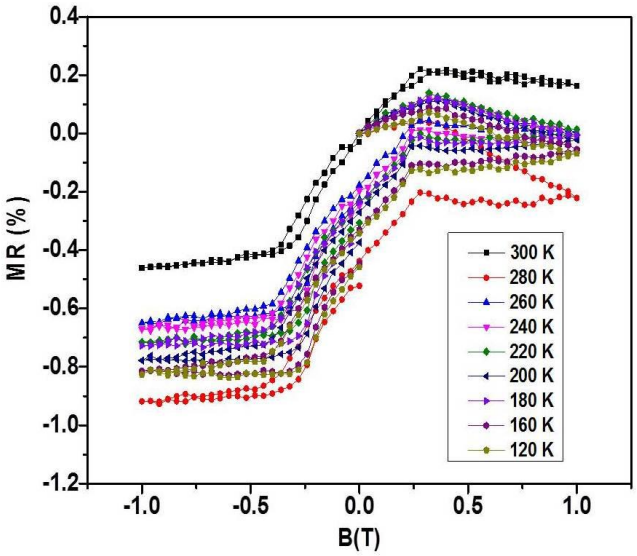

Fig. S3: Magnetoresistance as a function of magnetic field at various temperatures in the case of WT-bR spin valve

Control Experiments for MR Devices.

In order to confirm that the MR in our devices is not arising from the anomalous Hall effect in Ni contacts, 2-probe MR measurements was performed in the magnetic field out-of-plane of the device with a current of 50 μA at 100 K and is shown in Fig. S4. It can be seen that the behavior in 2-point measurement is dominated by contact resistance of Ni which shows anomalous MR. Clearly this behavior is symmetric to the applied field and very small ~ 0.03 % as compared to the value of MR we get in 4-point measurement. This proves that indeed MR in our devices is arising from junction which contains chiral molecules and is not related to anomalous behavior of Ni wire.

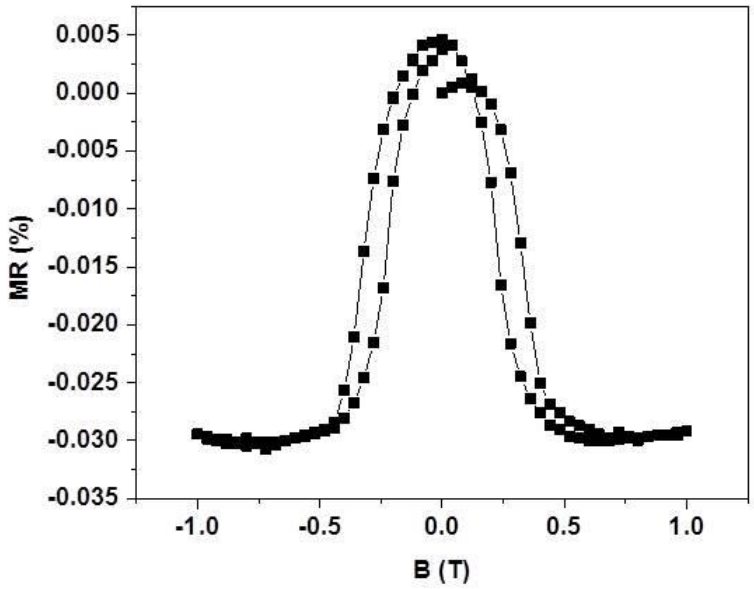

Fig. S4 2-probe MR measurement of the device at 100 K with magnetic field parallel to current i.e. out-of-plane direction.

The measurements were repeated many times and were found to be reproducible in Au/Cy/OTG-bR/MgO/Ni devices. Currents of 1 mA were applied, as mentioned in the manuscript, and the measured potential on the junction varied between 0.3-2 mV in the different devices. R(0) was calculated as the resistance at B=0. Fig. S5 illustrates the reproducibility of the MR results for different devices.

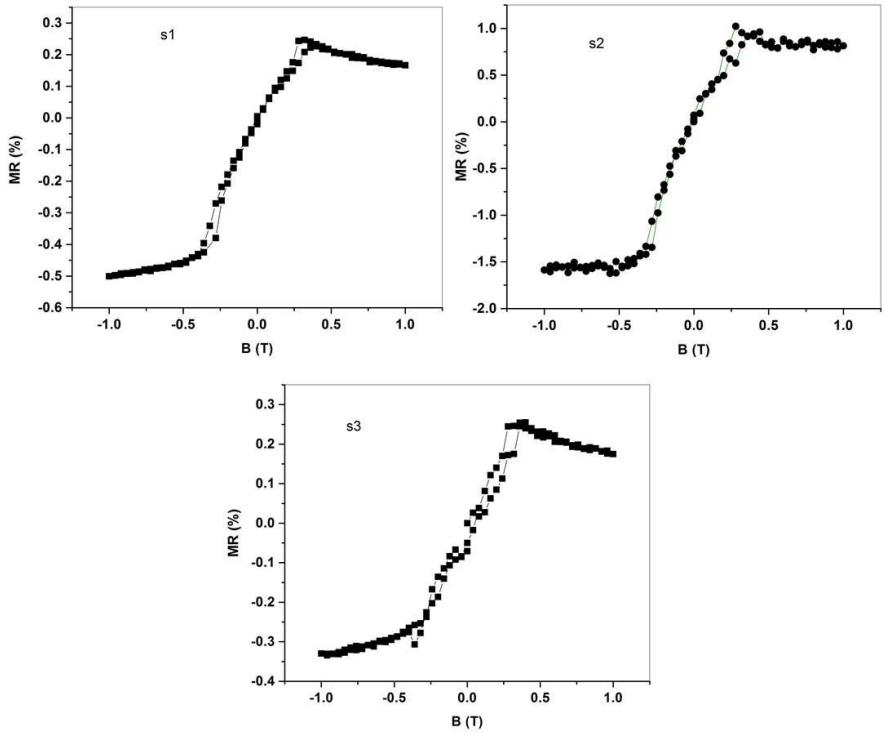

Fig. S5 MR curve for different devices s1, s2 and s3 at 300 K.

MR curves were also scanned continuously for different devices and were found to be quite stable and reproducible. Fig S6 shows 2 continuous scans for s0 (device from main manuscript) and s4.

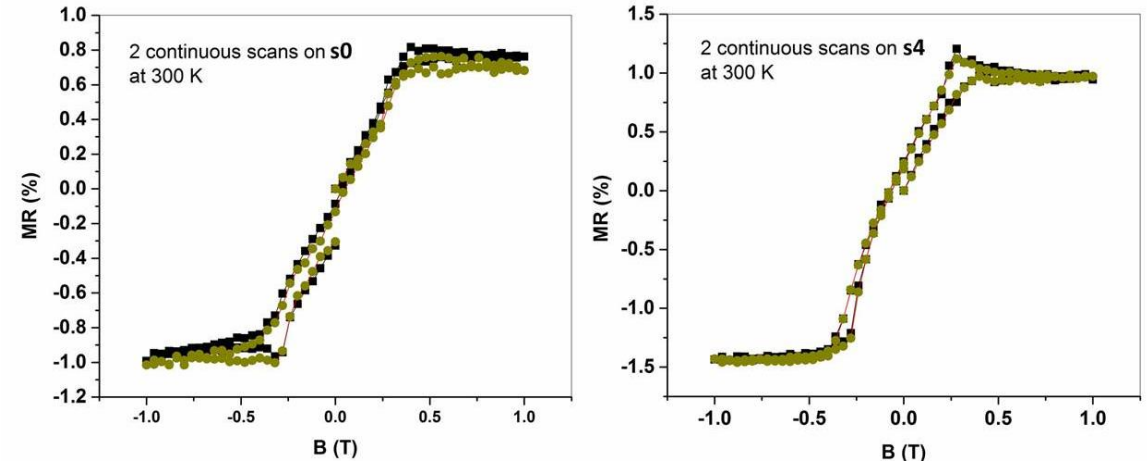

Fig. S6 Continuous scans for s0 and s4 devices at 300 K

Fig. S7 shows the MR scan at different currents on one of the device s5 at 300 K. It can be seen that the low current scan is slightly noisy but the features and value of the MR is same. The difference in absolute MR value, i.e. ~ 0.2 % at negative magnetic field and ~ 0.5 % at positive magnetic field may arise from a misalignment of the chiral molecules on the surface.

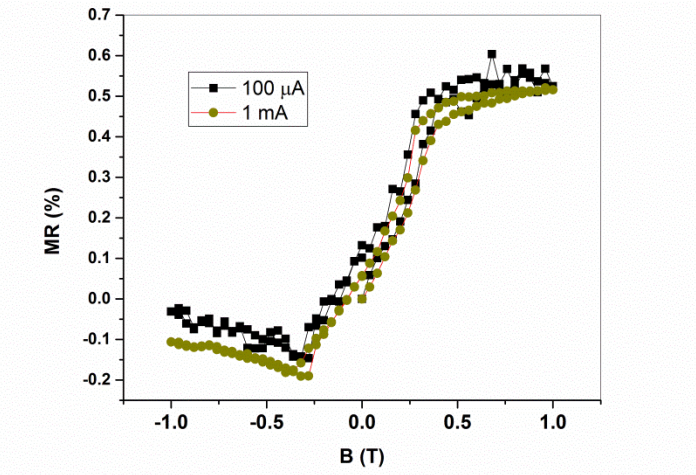

Fig. S7 MR curve for device s5 with different currents at 300 K